Nuclear Engineering and Technology 53 (2021) 2221–2228

Contents lists available at ScienceDirect

Nuclear Engineering and Technology

journal homepage: www.elsevier.com/locate/net

Original Article

Numerical study of oxygen transport characteristics in lead-bismuth eutectic for gas-phase oxygen control

Chenglong Wang [a, 1], Yan Zhang [a, 1], Dalin Zhang [a, *], Zhike Lan [b, **], Wenxi Tian [a], Guanghui Su [a], Suizheng Qiu [a]

[a] School of Nuclear Science and Technology, Xi'an Jiaotong University, Xi'an, 710049, China
[b] Nuclear Power Institute of China, Chengdu, 610005, China

ARTICLE INFO

Article history:
Received 27 September 2020
Received in revised form
17 January 2021
Accepted 28 January 2021
Available online 3 February 2021

Keywords:
Oxygen mass transfer
Gas-phase oxygen control
Mass transfer relation
Lead-bismuth eutectic (LBE)
CFD

ABSTRACT

One-dimensional oxygen transport relation is indispensable to study the oxygen distribution in the LBE-cooled system with an oxygen control device. In this paper, a numerical research is carried out to study the oxygen transport characteristics in a gas-phase oxygen control device, including the static case and dynamic case. The model of static oxygen control is based on the two-phase VOF model and the results agree well with the theoretical expectation. The model of dynamic oxygen control is simplified and the gas-liquid interface is treated as a free surface boundary with a constant oxygen concentration. The influences of the inlet and interface oxygen concentration, mass flow rate, temperature, and the inlet pipe location on the mass transfer characteristics are discussed. Based on the results, an oxygen mass transport relation considering the temperature dependence and velocity dependence separately is obtained. The relation can be used in a one-dimensional system analysis code to predict the oxygen provided by the oxygen control device, which is an important part of the integral oxygen mass transfer models.

1. Introduction

Lead-bismuth eutectic (LBE) is one of the candidate coolants of the Gen-IV reactors and accelerator-driven systems and has attracted worldwide attention in recent years. However, the corrosion of structural materials is a key problem that restricts the application of LBE. There are mainly two types of corrosion, dissolution corrosion and oxidation corrosion, which are influenced by the oxygen concentration in LBE [1]. Dissolution corrosion refers to that the alloying elements escape from the surface of the material and dissolve in the LBE under low oxygen concentration, which may make the thickness of stainless steel decreased and may lead to a phase transformation of stainless steel. When the oxygen concentration is high, the oxidation corrosion occurs and there are three ways of forming oxides: i) dissolved elements of the steel reacts with dissolved oxygen and form oxides; ii) elements of the steel (Fe) diffuses through the oxide layer and react with oxygen at steel surface to form outer oxide; iii) oxygen diffuses in the steel and form inner oxide (spinel Fe-Cr) [2,3].

Two corrosion mitigation strategies have been proved effective, including anti-oxidation coatings [4,5] and oxygen concentration control [6,7]. Among them, oxygen control is the most promising one because of the practical usefulness and good economy. With oxygen control techniques, oxygen concentration can be controlled in a range such that protective oxide layers will be formed and maintained on the surface of stainless steel to prevent further corrosion. And the oxygen concentration should also be controlled to prevent high corrosion rate and prevent lead oxide precipitation, which would lead to plugging of the loop [8]).

The most straightforward method for oxygen control is the use of oxygen and hydrogen gas mixture, known as the gas-phase oxygen control technique. When the oxygen in LBE is depleted or excessed as measured by the oxygen sensors, the oxygen or hydrogen is directly injected to the liquid or to the cover gas with an inert carrier gas to adjust the oxygen level. However, the partial pressure of oxygen in the gas mixture is relatively larger than the saturation partial pressure of oxygen in LBE, which would lead to the formation of the plugging or slag at the gas-liquid surface. To

* Corresponding author.
** Corresponding author.
E-mail addresses: xjyzhang@qq.com (Y. Zhang), dlzhang@mail.xjtu.edu.cn (D. Zhang), lanzhike@yahoo.com.cn (Z. Lan).
[1] These authors contributed equally to this article.

https://doi.org/10.1016/j.net.2021.01.031

solve the problem, another oxygen control method using the mixture of hydrogen and steam mixture is proposed, which could produce an extremely low oxygen concentration by the chemical equilibrium. The target partial pressure of oxygen can be obtained by controlling the ratio of the partial pressure of hydrogen and steam. However, whether the gas and steam can be adequately mixed and the required dimensions of the transfer device should be considered for industrial application [9].

Gas-phase oxygen control has been widely studied around the world and the research has gone through two stages, static research [10,11] and dynamic research [9,12], between which the difference is whether the LBE is stagnant or flowing. The oxygen transport in a stagnant system is only controlled by diffusion, which is not efficient enough to be applied to the industrial systems. As a result, the purpose of static research is to verify the feasibility of the technique and study the kinetics of the diffusion process. Dynamic research is designed to control the oxygen concentration in an LBE loop with higher efficiency and has been achieved on some facilities, including CORRIDA [9] in KIT, DELTA [13] in LANL.

The ongoing R&D activities on the oxygen control techniques mainly focus on the development of oxygen control systems and further corrosion test, while the attention on the kinetics of oxygen transport is less. To design an LBE-cooled reactor or experimental loop with an oxygen control system, the oxygen concentration distribution must be obtained. With a one-dimensional model for calculating the oxygen concentration change through an oxygen control system, the oxygen concentration distribution in the system can be obtained. Marino et al. [14] carried out experimental and numerical research on the solid-phase control and a relation between the Sherwood number and Peclet number was purposed. However, similar work is not reported for gas-phase control. As a result, numerical simulation on the gas-phase control is performed in this work to study the kinetics of oxygen transport in the oxygen control system and to provide a Sherwood number relation for gas-phase oxygen control.

In the first part of this paper, the models used in the simulation are introduced, including the theoretical models and numerical models. In the next two parts, the simulation results of static and dynamic oxygen control are reported, respectively. Finally, an oxygen transfer relation for dynamic oxygen control is obtained.

2. Oxygen transport models

2.1. Theoretical models

For turbulent flow, the transport equation for oxygen concentration is as follows:

$$\frac{\partial C_O}{\partial t}+\vec{u}.\nabla C_O=\nabla.\left(D+\frac{\mu_t}{Sc_t}\right)\nabla C_O+q_o \tag{1}$$

where C_o is the oxygen concentration, u is the velocity, D is the diffusion coefficient, μ_t is the eddy viscosity, Sc_t is the turbulent Schmidt number, and q_o is the oxygen provided by the cover gas or oxygen control device.

In the case of stagnant oxygen control and the oxygen concentration on the surface is assumed to be constant, the transport equation for oxygen concentration is simplified as:

$$\frac{\partial C}{\partial t}=D\frac{\partial^2 C}{\partial x^2} \tag{2}$$

Using the Laplace transformation, Crank gives a time-dependent solution for oxygen uptake or loss with a constant diffusion coefficient results [15] for Eq. (3), as follows:

$$\frac{M_t}{M_\infty}=1-\frac{8}{\pi^2}\sum_{n=0}^{\infty}\frac{1}{(2n+1)^2}\exp\left(-(2n+1)^2\pi^2\frac{Dt}{l^2}\right) \tag{3}$$

where M_t denotes the total amount of oxygen which has entered the LBE at time t and M_∞ the corresponding quantity after infinite time.

The diffusion coefficient and the solubility of oxygen in LBE are important properties to calculate the oxygen transport process. As suggested by the OECD, the diffusion coefficient and solubility of oxygen in LBE [16] are given by the two following expressions:

$$D_O\left(cm^2/s\right)=0.0239e^{-\frac{43073}{RT}}\quad 473\ \mathrm{K}<T<1273\ \mathrm{K} \tag{4}$$

$$\log(S,wt\%)=2.52-4803/T\quad 473\ \mathrm{K}<T<923\ \mathrm{K} \tag{5}$$

where D_O is the diffusion coefficient of oxygen in LBE in cm^2/s and R is the molar gas constant, 8.314 $J.K^{-1}mol^{-1}$, S is the solubility of oxygen in LBE in wt%.

The density and viscosity of LBE used in the study can also be found in Ref. [16].

2.2. Numerical models

The Volume of Fluid (VOF) model is used to build the gas-liquid interface in the simulation. The VOF model treats two or more immiscible fluids by solving a single set of momentum equations and tracking the volume fraction of each of the fluids throughout the domain. The volume fraction, γ, is adopted to indicate the distribution of the second phase. In the present study, the liquid LBE is set as the first phase, and the gas is set as the second phase. Therefore, the γ represents the volume fraction of the gas, as follows:

$$\begin{cases}\gamma=0 & The\,cell\,is\,full\,of\,LBE\\ 0<\gamma<1 & The\,cell\,contains\,the\,interface\,between\,the\,LBE\,and\,the\,gas\\ \gamma=1 & The\,cell\,is\,full\,of\,gas\end{cases} \tag{6}$$

The oxygen transport through the interface is modeled by adding a mass transfer source term to the conservation equations of mass fraction of fluids on both sides of the interface [17]:

$$\frac{\partial\left(\alpha_q\rho_q Y_q^i\right)}{\partial t}+\nabla.\left(\alpha_q\rho_q\overrightarrow{V_q}Y_q^i\right)=-\nabla.\left(\alpha_q\overrightarrow{J_q^i}\right)+\alpha_q R_q^i+\alpha_q S_q^i+\sum_n^{p=1}\left(\dot{m}_{p^iq^i}-\dot{m}_{p^iq^i}\right) \tag{7}$$

where p denotes the pth phase, n is the number of phases in the system. α_q, ρ_q and $\overrightarrow{V_q}$ are the phase volume fraction, density, and velocity for the qth phase. R_q^i and S_q^i are the net rates of production of species through chemical reaction and external sources. $\dot{m}_{p^iq^i}$ denotes the mass transfer source from species j on phase q to species i on phase p in $kg/(m^3.s)$. $\dot{m}_{p^iq^i}$ is defined similarly.

The mass transfer source is assumed to be a function of the mass concentration gradient of the transported species:

$$\dot{m}_{pq}=\dot{m}_{qp}=k_{pq}A_i\left(C_{q,e}-C_q\right) \tag{8}$$

where, k_{pq} is the volumetric mass transfer coefficient between phase p and phase q in m/s, A_i is the interfacial area concentration in m^{-1}, C_q is the mass concentration of oxygen in phase q, and $C_{q,e}$ is

the equilibrium mass concentration in kg/m^3.

The mass transfer coefficient k_{pq} can be obtained by the following expression:

$$k_{pq} = \frac{Sh_q D_q}{d_p} \tag{9}$$

where Sh_q is the Sherwood number of phase q, D_q is the diffusion coefficient of phase q in m^2/s and d_p is the bubble diameter of phase p in m.

The interfacial area concentration A_i is given by the following expression:

$$A_i = \frac{\alpha_p(1-\alpha_p)}{d_p} \tag{10}$$

where α_p is the volume fraction of phase p.

As mentioned above, there are two strategies for gas-phase control, O_2/H_2 or H_2/H_2O mixed with the inert carrier gas. For the former, the volume fraction of oxygen is directly set as inlet boundary conditions and for the latter, the oxygen is the production of the H_2O decomposition reaction. Practically, the H_2/H_2O mixture in the inlet is always fully mixed and is assumed to be in chemical equilibrium. The oxygen partial pressure is calculated using the following expression [8]):

$$\frac{1}{P^0}\frac{P_{H_2}^2 P_{O_2}}{P_{H_2O}^2} = K = \exp\left(12.894 - \frac{59273}{T}\right) \tag{11}$$

where T is the temperature in K, P^0 is the reference pressure in Pa, K is the equilibrium constant, and P_{H_2}, P_{O_2}, and P_{H_2O} are the partial pressures of H_2, O_2, and H_2O, respectively.

When the oxygen is not saturated in LBE, the oxygen partial pressure in equilibrium with the dissolved oxygen in liquid LBE can be written as a function of oxygen concentration and temperature [8]) according to:

$$P_{O_2} \Big/ bar = C_O^2 \exp\left(13.558 - \frac{32005}{T}\right) \tag{12}$$

All the above equations and relations are solved using the ANSYS Fluent software. The VOF model is used to calculate the two-phase interface and the species transport model with UDFs (User-Defined Functions) is used to calculate the oxygen transport in LBE. The influence of dissolved oxygen on the physical properties of LBE is neglected as the oxygen concentration is small. The liquid in this simulation is assumed to be isothermal.

3. Static oxygen control

For the validation of the oxygen diffusion models, a transient simulation is carried out. A rigid plane of stagnant LBE with a height of l is assumed and the oxygen pressure on the upper surface is assumed to be constant. Based on the results, the relation between $\frac{M_t}{M_\infty}$ and $\frac{Dt}{l^2}$ is drawn in Fig. 1. The results show a good agreement with Eq. (3). The temperature of the simulation is 500 °C.

A container with an inlet and outlet is developed as the geometry for the study of stagnant oxygen control, as shown in Fig. 2. In the simulation, LBE is kept stagnant in the lower region of the container and the gas mixture enters the system from the inlet and escapes from the pressure outlet to investigate the oxygen transport characteristics from the gas phase to LBE. The temperature of the simulation is 500 °C.

Two kinds of control strategies are considered in the simulation

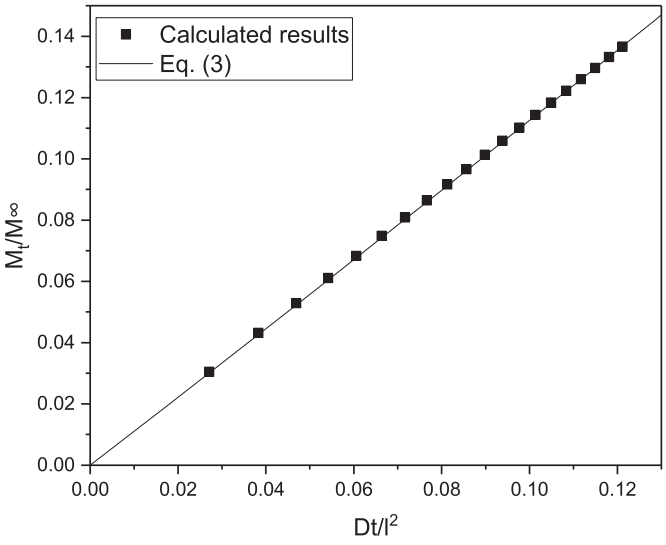

Fig. 1. Validation of the diffusion model.

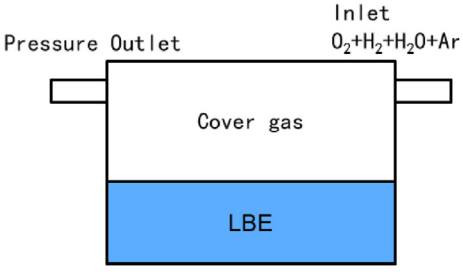

Fig. 2. Geometry for static gas-phase oxygen control.

including H_2+O_2 and H_2+H_2O, both with Argon as the carrier gas. For the control using H_2+O_2, the inlet oxygen volume fraction in the gas mixture is 0.02. At the initial time, the oxygen fraction in the cover gas is 0.02 and the oxygen concentration in LBE is 0. The change of oxygen concentration in LBE with time is shown in Fig. 3 and the detailed oxygen concentration changes at different heights are shown in Fig. 4. The area between the two blue dash lines in Fig. 4 refers to the range of typical target operating oxygen concentration and it is similar in Fig. 5. According to the results, the oxygen equilibrium between the gas and LBE around the interface is established immediately when the gas is contacted with LBE and the oxygen concentration at the interface reached saturated within 1 s. The oxygen diffusion from the interface to the bulk liquid is relatively slower compared to the transport through the interface. In general, the oxygen supplementation using O_2 is fast and the oxygen concentration in the bulk liquid reached more than 1×10^{-8} wt%, which is a general oxygen lower limitation in the LBE system, within 100 s. However, one problem observed in the results is the highly non-uniformed oxygen distribution especially around the interface. The accumulation of oxygen around the interface may lead to the creation of PbO and may cause corrosion to the neighboring container wall.

The change of oxygen concentration in the oxygen control process using H_2+H_2O is shown in Fig. 5. The advantage of this strategy is that the partial pressure of oxygen in the gas mixture could be extremely low and therefore the non-uniform distribution could be eliminated. In this simulation, the volume fraction of H_2 in the gas mixture is 0.0015, the H_2O fraction is 0.0105 and the volume fraction ratio of H_2/H_2O is 0.143. The inlet oxygen partial pressure is

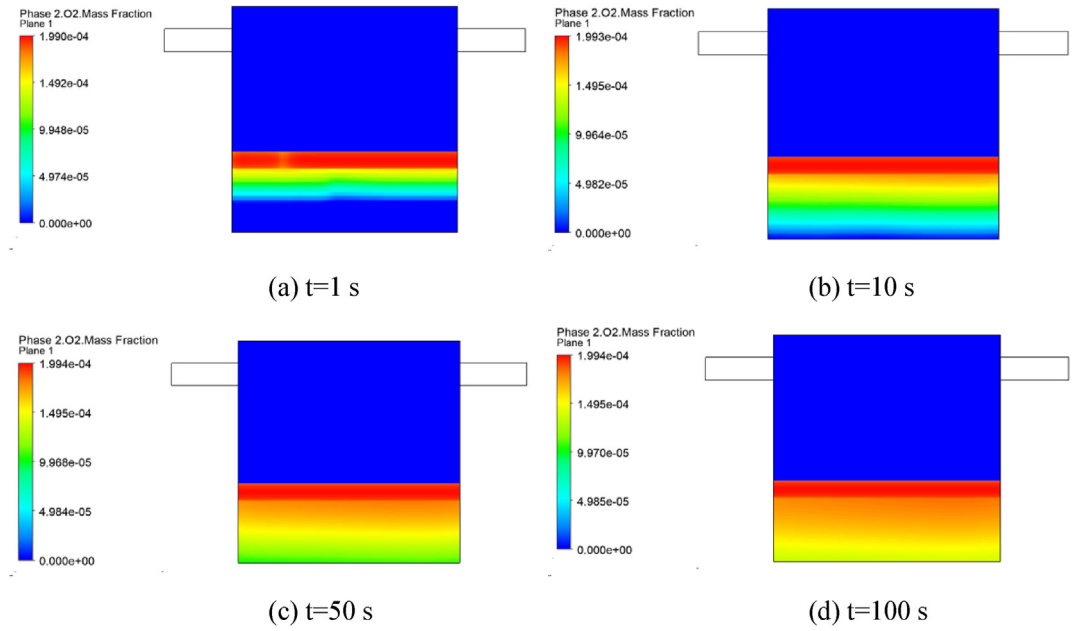

Fig. 3. The oxygen concentration change with time.

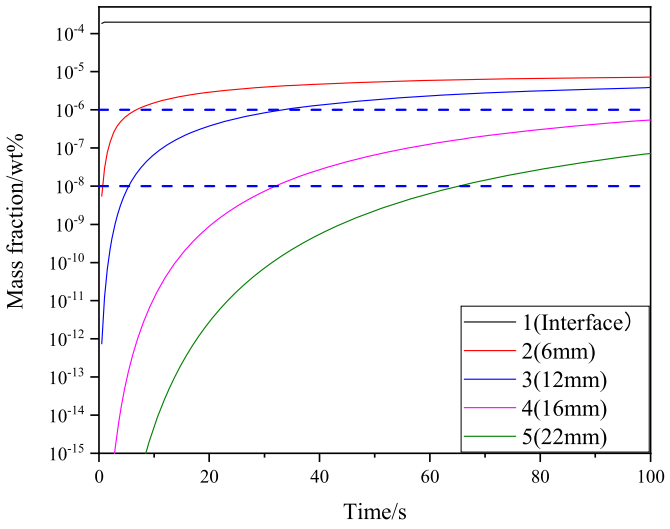

Fig. 4. Oxygen concentration at different positions in the control using O_2+H_2.

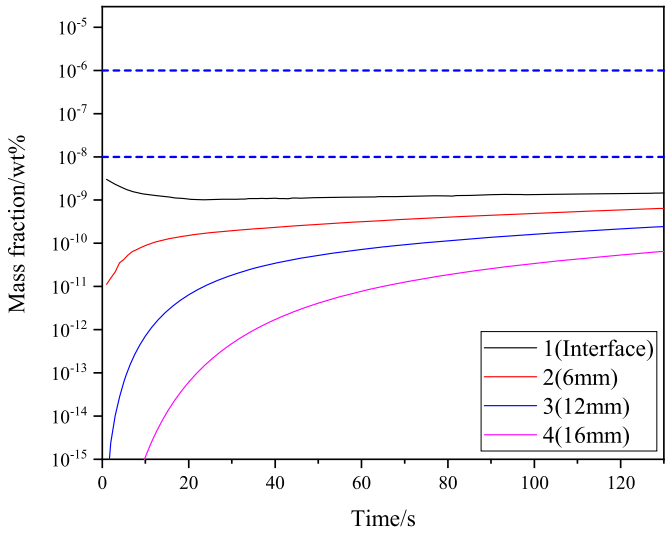

Fig. 5. Oxygen concentration at different positions in the control using H_2+H_2O.

then calculated by Eq. (7), resulting in 9.72×10^{-22} *Pa* and the initial oxygen partial pressure in the cover gas is also set as 9.72×10^{-22} *Pa*. According to the results, the oxygen concentration at the interface increases sharply when the gas is contacted with LBE and the oxygen equilibrium between the gas mixture and LBE is also established within 1 s. After the first second, the oxygen concentration begins to decrease because the oxygen in the gas side around the interface is depleted and the followed supplementation from the inlet has not arrived. When the inlet gas reached the interface at about t = 20 s, the oxygen concentration in LBE increases again. It can be observed that the oxygen concentration distribution is more uniform than the control using O_2+Ar. However, the spent time to reach the target operating oxygen concentration is obviously longer, which can be improved by adopting dynamic oxygen control.

4. Dynamic oxygen control

4.1. Geometry and boundary conditions

The simulation geometry for dynamic gas-phase oxygen control is developed referring to the oxygen transfer device of the CORRIDA loop in KIT, as shown in Fig. 6 [12]. The oxygen transfer device is a horizontal tube with an inner diameter of 305 mm and a length of 1100 mm. In this paper, the simulation geometry is a 1:10 scaled model. The LBE contacts with the gas directly in the device and the filling level of LBE is about 1/3 of the height, which resulting in a contacted area of 3111 mm^2. In the experimental conditions, the volume flow rate of the pre-mixed gas is 500 cm^3/min, resulting in the flow velocity of less than 1 mm/s and residence time at 550°*C* of 2500 s. Relatively, the residence time of the LBE in the vessel is 44 s, corresponding to a flow velocity of 25 mm/s. As a result,

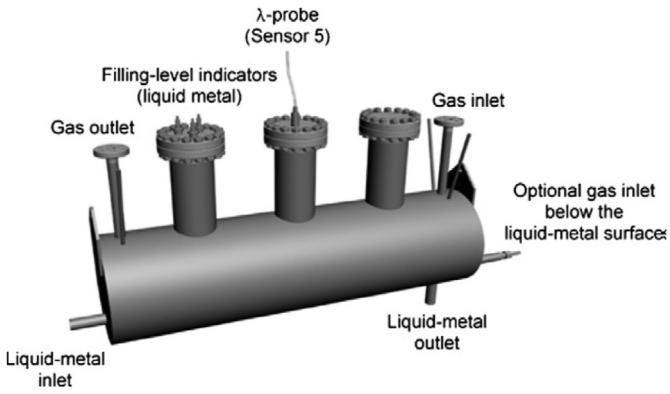

Fig. 6. Oxygen control device of the CORRIDA loop.

compared with LBE flow, the gas atmosphere inside the transfer device is quasi-stagnant [12].

According to the study on the kinetics of oxygen transport in the static oxygen control and some literature, following assumptions are made for the model of dynamic gas-phase oxygen control:

- The gas inside the transfer device is quasi-stagnant compared with LBE flow and the gas-LBE interface is assumed to be stable.
- Oxygen consumption in the transfer device is low so that the gas composition is assumed to be the same from the inlet to the outlet [9].
- Oxygen transport through the interface is sufficiently fast as shown in the static gas-phase control.

Besides, the oxygen diffusion coefficient in the gas phase is two orders of magnitude than in the LBE [16,18]. In conclusion, the oxygen concentration at the interface is assumed to be a constant as long as the gas supplementation is steady. Based on the assumptions, the gas phase is not modeled in the simulation and the gas-LBE interface is treated as a free-surface boundary with constant oxygen concentration. The interface concentration is used to simulate the oxygen source from the gas phase that is not modeled. When the gas is Ar/O_2, the interface oxygen concentration is the solubility limit. When dealing with the $Ar/H_2/H_2O$ case, the interface oxygen concentration is calculated using Eq. (11) and Eq. (12) and the gas is assumed to be in equilibrium.

The computational domain is shown in Fig. 7. The structured mesh is adopted to reduce the amount of mesh and to improve the convergence. After the mesh independence analysis, the minimum mesh size is set as 2×10^{-4} m and the total number of the elements is about 3,500,000. The simulation conditions are designed according to the experimental conditions in the CORRIDA experiment and expanded to cover the working conditions of the general LBE-cooled system, as listed in Table 1.

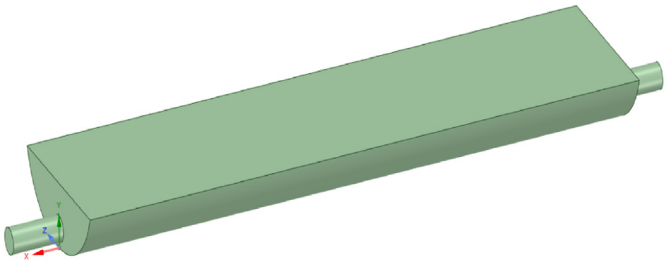

Fig. 7. The computational domain of dynamic gas-phase oxygen control.

Table 1
Simulation conditions of dynamic gas-phase oxygen control.

Parameters	Values
Temperature of LBE (°C)	350, 400, 450, 500, 550
Mass flow rate of LBE (kg/s)	0.05, 0.1, 0.15, 0.2
Inlet oxygen concentration (wt%)	1.10^{-6}, 5.10^{-6}
Interface oxygen concentration (wt%)	1.10^{-5}, 1.10^{-4}, ..., the solubility

4.2. Results analysis

The oxygen concentration and velocity distribution at a cross-section of the oxygen transfer device for the condition $T_{in} = 450\ ^{\circ}C$ and $\dot{m} = 0.1$ kg/s are shown in Fig. 8. According to the results, the oxygen concentration increases with the LBE flowing from inlet to outlet and the corresponding oxygen transfer rate decreases. The profile of oxygen concentration and velocity show high consistency especially near the liquid metal inlet region, where the reversed flow exists. Since oxygen concentration at the interface is much larger than that inside the container, the reversed flow can therefore mix the oxygen quickly and enhance the oxygen transport.

To quantitatively study the efficiency of the oxygen control device, some variables should be defined. The average dissolution rate represents the quantity of oxygen taken by the flowing LBE in a limited time and is determined as follows:

$$q = \dot{m}(C_{out} - C_{in}) \tag{13}$$

where q is the average dissolution rate in kg/s, $\dot{m}$ is the mass flow rate in kg/s, C_{out} and C_{in} are the average oxygen concentration at the outlet and inlet in wt%, respectively.

The average mass transfer coefficient is then calculated using the dissolution rate:

$$k = \frac{q}{A(C_s - C)} \tag{14}$$

where k is the mass transfer coefficient in $kg/(m^2.s)$, A is the area of gas-liquid interface in m^2, C_s is the oxygen concentration at the interface and C is the bulk concentration, which is calculated by the average oxygen concentration of the inlet and outlet.

Sherwood number represents the ratio of the convective mass transfer to the rate of diffusive mass transport. In this study, the Sherwood number is defined as follows:

$$Sh = \frac{K.l}{\rho.D} \tag{15}$$

where l is the characteristic length in m.

The other non-dimensional numbers include the Reynolds number, the Schmidt number, and the Peclet number, defined as:

$$Re = \frac{ul}{\nu} \tag{16}$$

$$Sc = \frac{\nu}{D} \tag{17}$$

$$Pe = Re.Sc \tag{18}$$

where u is the inlet velocity in m/s, ν is the kinematic viscosity in m^2/s.

4.2.1. Parameter sensitivity analysis

With a given temperature, T = 550°C, oxygen transport at

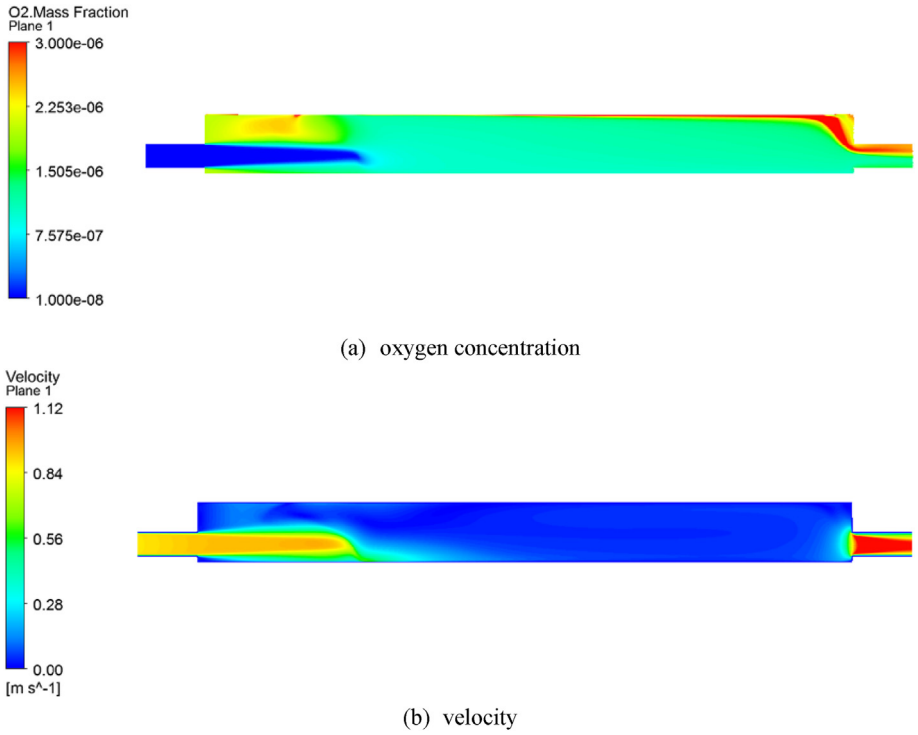

Fig. 8. Oxygen concentration and velocity profiles (T_{in} = 450 °C $\dot{m}$ = 0.1 kg/s).

different inlet mass flow rates, different oxygen concentrations at the inlet and the interface are compared. The mass transfer coefficients obtained from the cases are shown in Fig. 9. As shown in the results, the mass transfer coefficient increases with mass flow rate because of the increased turbulent intensity, which helps to improve the effect of convection in oxygen transport. On the other hand, the influence of oxygen concentration at the inlet and the interface on the mass transfer coefficient is negligible, which proves that the oxygen transport is influenced only by the temperature and flow conditions. The conclusion also provides the feasibility of a Sherwood number relation, from which the outlet oxygen concentration could be obtained with the inlet and interface oxygen concentration and the flow conditions.

The influence of the temperature on the mass transfer coefficient is shown in Fig. 10. According to the results, the mass transfer coefficient increases with the increase of temperature and the increasing slope becomes steeper at a higher mass flow rate. With the increase of temperature, the viscosity of LBE decreases and the diffusion coefficient increases. The oxygen transport in LBE is influenced by two processes, diffusion and convection. The decrease of viscosity will lead to an increase in Re number and turbulence intensity, which eventually make the convection process improved. In the meanwhile, the increase in the diffusion coefficient directly makes the diffusion process enhanced. In

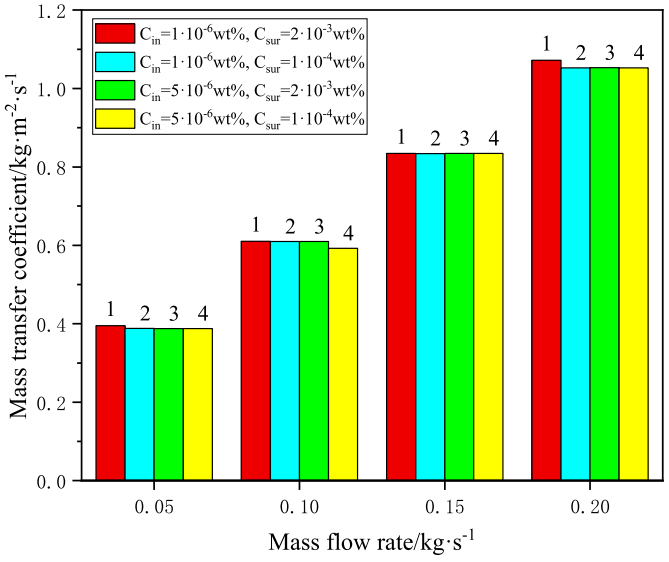

Fig. 9. Results of different mass flow rate, inlet and interface oxygen concentration.

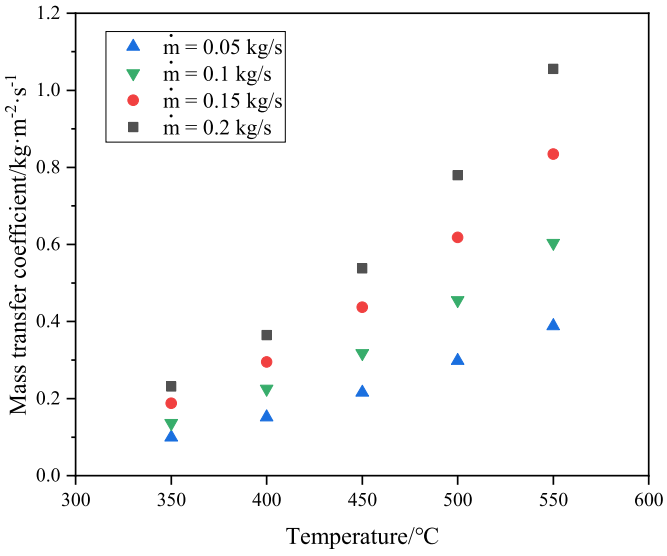

Fig. 10. Influence of temperature on the mass transfer coefficient.

conclusion, the oxygen mass transfer is enhanced under the combined effects of the two sides. On the other hand, as shown in Fig. 10, when the temperature is fixed, the mass transfer coefficient increases with the mass flow rate. As the mass flow rate increases, the Re number becomes larger and turbulence mixing in the bulk liquid is enhanced, which makes the convection effect in the mass transfer process larger. As a result, the mass transfer coefficient of LBE increases.

As mentioned above, the oxygen transport can be significantly improved by the reversed flow around the LBE inlet region, which is mainly influenced by the mass flow rate and the location of the inlet pipe. Since the location of the inlet pipe is not specified in the description of the CORRIDA loop, three geometries with different locations of inlet pipe are developed to study the influence of inlet location on the mass transfer. The change of the Sh number with the same *Pe* number and different inlet pipe location is shown in Fig. 11. According to the results, the oxygen transfer enhances with higher inlet pipe location, the main reason for which is the change of flow conditions around the reversed flow region. However, it is difficult to quantitatively assess the influence of the inlet pipe location and the analysis should be made respectively for each oxygen transfer device design.

4.2.2. Relation fitting

The ultimate target of this study is to obtain the relation for Sh number, which could be used in a one-dimensional code. Generally, the mass transfer relation could be fitted following two formulas, as shown in Eq. (19) and Eq. (20). All the results obtained from the simulation are drawn in Fig. 12 and two relations based on the two formulas are fitted, as shown in Table 2. According to the results, the deviation of the parameters in Eq. (19) is relatively large compared with the one in Eq. (20). In the meanwhile, as shown in Fig. 12, the influences of temperature and velocity are on different levels, which means that the exponents of the Re number and Sc number in the relation should be different. Consequently, the temperature dependence (Sc) and velocity dependence (Re) are considered in the relation separately to better describe the data. The improved relation is shown as Eq. (21) and the comparison between two relations is shown in Fig. 13. The improved relation shows an obvious superiority over the original one.

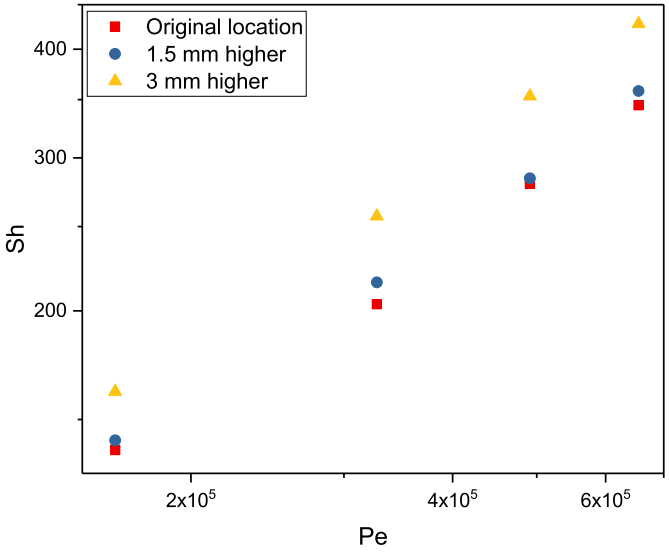

Fig. 11. Comparison of different inlet pipe locations.

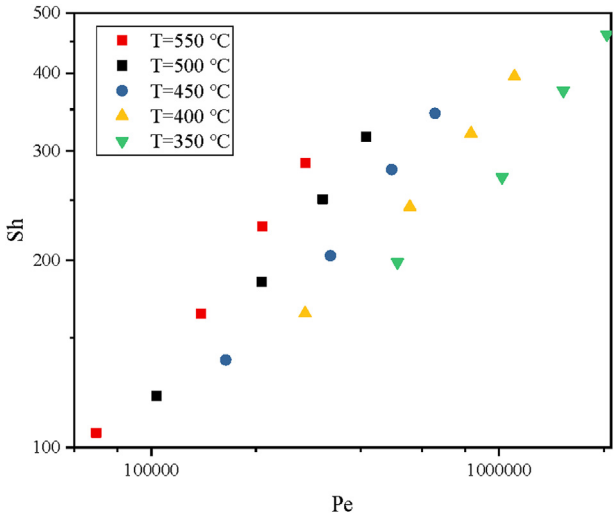

Fig. 12. The relation between the Sherwood number and Peclet number.

Table 2
Fitted parameters of oxygen mass transfer relation.

Parameters	A	B	C
Eq. (19)	1.95119±1.15939	0.37386±0.04364	–
Eq. (20)	0.23568±0.15547	0.68111±0.06768	0.25859±0.03402

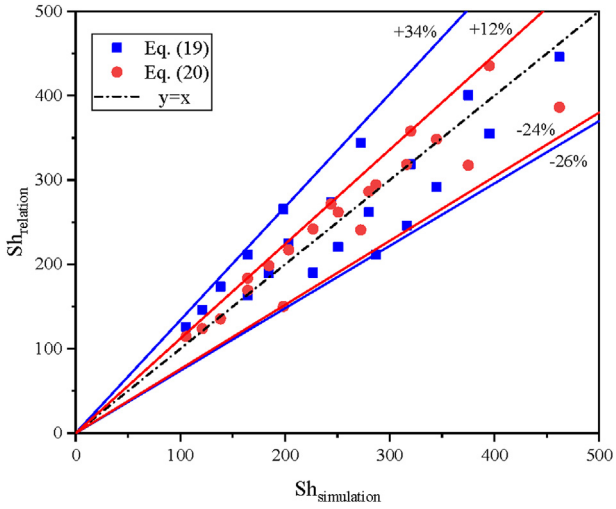

Fig. 13. Comparison between two relations.

$$Sh = A.Pe^{B} \tag{19}$$

$$Sh = A.Re^{B}.Sc^{C} \tag{20}$$

$$Sh = 0.23568.Re^{0.68111}.Sc^{0.25859} \quad 1850 < Re < 995028 < Sc < 275 \tag{21}$$

5. Conclusions

In this study, oxygen transport characteristics in LBE for gas-phase oxygen control is investigated. The research consists of two

parts, static oxygen control and dynamic oxygen control. The model of the static oxygen control is based on the two-phase VOF model and the results are in good agreement with the theoretical expectations. The model of dynamic oxygen control is a single-phase simulation, aiming to establish an oxygen mass transport relation for a gas-phase oxygen control device. The main conclusions are as follows:

1) According to the results of static oxygen control simulation, the control strategy using H_2+H_2O provides a more uniform oxygen distribution and a longer controlling time compared with the one using H_2+O_2.
2) For the dynamic oxygen control, oxygen transport is dominated mainly by the convection, which is proved by the high consistency between the oxygen concentration and velocity profiles.
3) The mass transfer coefficient does not change with inlet and interface concentrations, increases with the increase of mass flow rate and temperature. The location of the inlet pipe has an influence on the oxygen mass transport and the influence level should be analyzed case by case.
4) An oxygen mass transport relation for a gas-phase oxygen control device considering the temperature dependence and velocity dependence separately is obtained:

$$\begin{aligned} &\mathrm{Sh} = 0.23568.\mathrm{Re}^{0.68111}.Sc^{0.25859} \\ &1850 < Re < 995028 < Sc < 275 \end{aligned} \tag{22}$$

Although the diffusion model is validated by the theoretical solution, some models cannot be validated because of the lack of experimental data, including the mass transport models through the gas-LBE interface and the assumptions for dynamic oxygen control. The attention on the oxygen transport characteristics in LBE is still insufficient and more experimental and numerical research is needed.

Declaration of competing interest

The authors declare that they have no known competing financial interests or personal relationships that could have appeared to influence the work reported in this paper.

Acknowledgments

Financial support for this work was provided by the National Natural Science Foundation of China (No. 11675162) and the National Key Research and Development Program of China (No. 2019YFB1901300).

References

[1] Y. Zhang, C. Wang, Z. Lan, S. Wei, R. Chen, W. Tian, G. Su, Review of thermal-hydraulic issues and studies of lead-based fast reactors, Renew. Sustain. Energy Rev. 120 (2020).
[2] R.G. Ballinger, J. Lim, An overview of corrosion issues for the design and operation of high-temperature lead- and lead-bismuth-cooled reactor systems, Nucl. Technol. 147 (2017) 418–435.
[3] L. Martinelli, K. Ginestar, V. Botton, C. Delisle, F. Balbaud-Célérier, Corrosion of T91 and pure iron in flowing and static Pb-Bi alloy between 450 °C and 540 °C: experiments, modelling and mechanism, Corrosion Sci. 176 (2020).
[4] Y. Kurata, H. Yokota, T. Suzuki, Development of aluminum-alloy coating on type 316SS for nuclear systems using liquid lead–bismuth, J. Nucl. Mater. 424 (2012) 237–246.
[5] I. Proriol Serre, I. Diop, N. David, M. Vilasi, J.B. Vogt, Mechanical behavior of coated T91 steel in contact with lead–bismuth liquid alloy at 300°C, Surf. Coating. Technol. 205 (2011) 4521–4527.
[6] G. Muller, A. Heinzel, J. Konys, G. Schumacher, Results of steel corrosion tests in flowing liquid Pb/Bi at 420–600 °C after 2000 h, J. Nucl. Mater. 301 (2002) 40–46.
[7] C. Schroer, J. Konys, T. Furukawa, K. Aoto, Oxidation behaviour of P122 and a 9Cr–2W ODS steel at 550°C in oxygen-containing flowing lead–bismuth eutectic, J. Nucl. Mater. 398 (2010) 109–115.
[8] C. Schroer, J K, Physical Chemistry of Corrosion and Oxygen Control in Liquid Lead and Lead-Bismuth Eutectic, 2007.
[9] C. Schroer, O. Wedemeyer, J. Konys, Gas/liquid oxygen-transfer to flowing lead alloys, Nucl. Eng. Des. 241 (2011) 1310–1318.
[10] K. Lambrinou, E. Charalampopoulou, T. Van der Donck, R. Delville, D. Schryvers, Dissolution corrosion of 316L austenitic stainless steels in contact with static liquid lead-bismuth eutectic (LBE) at 500 °C, J. Nucl. Mater. 490 (2017) 9–27.
[11] C.H. Lefhalm, J. Knebel, K.J. Mack, Kinetics of gas phase oxygen control system (OCS) for stagnant and flowing Pb–Bi Systems, J. Nucl. Mater. 296 (2001) 301–304.
[12] L. Brissonneau, F. Beauchamp, O. Morier, C. Schroer, J. Konys, A. Kobzova, F. Di Gabriele, J.L. Courouau, Oxygen control systems and impurity purification in LBE: learning from DEMETRA project, J. Nucl. Mater. 415 (2011) 348–360.
[13] N. Li, V. Tcharnotskaria, T. Darling, C. Ammerman, X. He, J. King, D. Harkleroad, Lead-bismuth Eutectic (LBE) Materials Test Loop (MTL) Test Plan. LA-UR-01-4866, 2001.
[14] A. Marino, J. Lim, S. Keijers, S. Vanmaercke, A. Aerts, K. Rosseel, J. Deconinck, J. Van den Bosch, A mass transfer correlation for packed bed of lead oxide spheres in flowing lead–bismuth eutectic at high Péclet numbers, Int. J. Heat Mass Tran. 80 (2015) 737–747.
[15] J. Crank, The Mathematics of Diffusion, second ed., Clarendon, Oxford, 1975.
[16] Oecd, Handbook on Lead-bismuth Eutectic Alloy and Lead Properties, Materials Compatibility, Thermalhydraulics and Technologies, Organisation for Economic Co-Operation and Development, 2015.
[17] ANSYS, ANSYS Fluent Theory Guide, 2016.
[18] E.N. Fuller, P.D. Schettler, J.C. Giddings, New method for prediction of binary gas-phase diffusion coefficients, Ind. Eng. Chem. 58 (1966) 18–27.